Virology 401 (2010) 322–332

Contents lists available at ScienceDirect

Virology

journal homepage: www.elsevier.com/locate/yviro

Role of individual caspases induced by astrovirus on the processing of its structural protein and its release from the cell through a non-lytic mechanism

Ma. del Rocío Banos-Lara, Ernesto Méndez *

Departamento de Genética del Desarrollo y Fisiología Molecular, Instituto de Biotecnología, Universidad Nacional Autónoma de México, Avenida Universidad 2001, Colonia Chamilpa, Cuernavaca, Morelos, 62210, México

ARTICLE INFO

Article history:
Received 17 November 2009
Returned to author for revision
13 December 2009
Accepted 23 February 2010
Available online 29 March 2010

Keywords:
Astrovirus
Virus release
Capsid protein processing
Caspases

ABSTRACT

Caspases (*Casp*) activity has been associated with the intracellular proteolytic processing of the structural protein to yield the mature capsid formed by VP70 and with the cell release of human astrovirus (HAstV). This work describes the role of individual *Casp* on these events. The activity of initiator (*-8*, *-9*) and executioner (*-3*/*7*) *Casp* was clearly detected at 12 h post-infection. All these proteases were able to cleave VP90 in an *in vitro* assay, but this processing was blocked in cells transfected with siRNA against *Casp-3*, *-9*, but not against *Casp-8*. In contrast, virus release, observed in the absence of cell lysis, was more drastically affected by either silencing *Casp-3* or in the presence of the inhibitor Ac-DEVD-CHO. Cleavage of VP90 to yield VP70 was mapped at motif $TYVD_{657}$. These data indicate that the processing of VP90 and the release of HAstV from the cell are two *Casp*-related, but apparently independent, events.

Introduction

Human astroviruses (HAstV) are etiological agents of viral diarrhea in young children and immunocompromised patients (Gallimore et al., 2005; Mendez and Arias, 2007). Eight genotypes/serotypes of HAstV generally present among human population have been described (Koopmans et al., 1998; Taylor et al., 2001); however, recent reports revealed the presence of astroviruses (AstV), less related to the HAstV serotypes previously described, in children; their clinical relevance is still being investigated (Finkbeiner et al., 2009). AstV have also been identified in a variety of animal species, causing several diseases, besides gastroenteritis (Baxendale and Mebatsion, 2004; Behling-Kelly et al., 2002). Viruses included into the Astroviridae family are non-enveloped icosahedral virus of around 40 nm in diameter, including spikes, and they can be observed as star-like structures in stool samples (Mendez and Arias, 2007). Their genome is formed by a single-stranded RNA molecule of plus polarity that contains three open-reading frames (ORF), named ORF1a, ORF1b, and ORF2. ORF1a and ORF1b code for proteins that contain motifs of a serine-protease and the RNA-dependent RNA polymerase, respectively (Jiang et al., 1993). The non-structural proteins nsp1a and nsp1ab are synthesized from these ORFs and are cleaved by at least one cellular protease and the viral protease (Geigenmuller et al., 2002; Mendez et al., 2003). On the other hand, ORF2 codes for a protein of 87–90 kDa (named VP90 in HAstV-8) that represents the capsid precursor polypeptide (Mendez et al., 2002; Monroe et al., 1993; Willcocks and Carter, 1993). VP90 contains at least three domains distinguishable by their sequence identity: a highly conserved amino terminal domain (residues 1 to 415), a highly divergent intermediate domain (residues 416 to about 647), and the carboxy-end domain, which is also highly variable (648 to the end) (Jonassen et al., 2001; Mendez-Toss et al., 2000; Wang et al., 2001). In spite of their low identity, the last 130 residues of the protein are highly conserved in the acidic character (Mendez et al., 2004). An intracellular proteolytic processing of particles containing VP90 to yield particles formed by a 70-kDa protein (VP70), which has been related with the maturation of HAstV-8 virions, occurs in this region, and the aspartic acid residues seem necessary for that processing (Mendez et al., 2004). Viral particles containing VP70 are further on extracellularly cleaved by trypsin to generate particles with high infectivity, formed by three proteins of 34, 27, and 25 kDa (named VP34, VP27, and VP25, respectively) (Mendez et al., 2002). The mechanism by which infectivity is enhanced due to trypsin treatment is still unknown.

Apoptosis is one type of programmed cell death, involved in many cellular processes (Doseff, 2004; Hildeman et al., 2007). Particularly, it has been considered as a cell response to viruses infection in order to block their replication (Barber, 2001); however, these pathogens have evolved mechanisms to avoid or modulate that response to successfully complete their replication cycle (McLean et al., 2008). Caspases (*Casp*) are cystein-proteases specific for aspartic acid residues that play a key role in this kind of cell death. These enzymes can be activated (by proteolysis), by a variety of stimuli, including

* Corresponding author. Departamento de Genética del Desarrollo y Fisiología Molecular, Instituto de Biotecnología, Universidad Nacional Autónoma de México, Apartado Postal 510-3, Colonia Miraval, Cuernavaca, Morelos, 62250, México. Fax: +52 777 3291622.
E-mail address: ernesto@ibt.unam.mx (E. Méndez).

0042-6822/$ – see front matter © 2010 Elsevier Inc. All rights reserved.
doi:10.1016/j.virol.2010.02.028

ligands to death receptors and cytotoxic drugs (Bertrand et al., 1994; Schulze-Osthoff et al., 1998). At least two different groups of *Casp* involved in cell death have been recognized, depending on how they are activated: initiator (such as *Casp-8*, *-9*, and *-4*, among others) and executioner (such as *Casp-3* and *-7*, among others). Initiator *Casp* are usually self-activated when cells sense the stimulus by forming protein complexes, whose composition and cell localization depend on the stimuli (MacFarlane, 2003; Riedl and Salvesen, 2007). Two classical pathways involved in the activation of initiator *Casp* are recognized: (a) the extrinsic pathway that frequently results in the activation of *Casp-8* (or *Casp-10*) is usually initiated by an extracellular signal that recognizes death receptors on the membrane. Ligands, such as tumor necrosis factor (TNF) or TNF-related apoptosis ligand (TRAIL), are examples of extrinsic pathways activators. (b) The intrinsic pathway is frequently initiated by genotoxic stress caused by drugs such as staurosporine and results in the activation of *Casp-9*. This *Casp* forms complexes with mitochondrial factors for its self-activation (Fuentes-Prior and Salvesen, 2004; Wang et al., 2005). xA third route of *Casp* activation triggered by stress in the endoplasmic reticulum (ER) has been recognized (Rao et al., 2001). In this case, *Casp-4* in human (Hitomi et al., 2004a) and *Casp-12* in mice cells (Hitomi et al., 2004b; Nakagawa et al., 2000) are the initiator *Casp*, and agents such as thapsigargin or tunicamycin can activate them (Hu et al., 2004). After initiator *Casp* are activated by self-cleavage, these proteases cleave and activate executioner proteases, such as *Casp-3*, *-6*, and *-7* (Inoue et al., 2009). Executioner *Casp* are mostly responsible for the cleavage of cellular proteins with structural or enzymatic activities, taking the cell to dramatic alterations and death (Fischer et al., 2003; Taylor et al., 2008).

Alterations associated with cell death by apoptosis, including cleavage of cellular structural proteins and of the *pro-Casp-8* (*pCasp-8*) at late times post-infection, have been observed in HAstV-infected Caco-2 cells (Guix et al., 2004a; Mendez et al., 2004). Indirect observations have related *Casp* activity with the release of the virus from the cell (Guix et al., 2004a; Mendez et al., 2004) and with the processing of VP90 to VP70 (Mendez et al., 2004). Both events are enhanced by TRAIL and blocked by the pan-*Casp* inhibitor Z-VAD-fmk (Mendez et al., 2004). Although *Casp-8* was found cleaved 48 h post-infection (hpi) upon HAstV-4 infection (Guix et al., 2004a), no individual *Casp* has been associated with virus release and VP90 cleavage, since at that time of infection these events had already occurred (Mendez et al., 2004). Cleavage of VP90 seems to be necessary for virus release, but not for viral particles assembly, since infectious particles can be rescued from cells kept in presence of Z-VAD-fmk (Mendez et al., 2007). Thus, the mechanism by which VP90 is cleaved by *Casp* and the specific *Casp* responsible for that cleavage are unknown. This work was carried out to understand better the relationship between the cell response to HAstV infection that results in individual *Casp* activation and the effect of each of these proteases on VP90 cleavage and astrovirus release from the host cell.

Results

Intracellular proteolytic processing of VP90 coincides with the release of astrovirus and the executioner Casp activity

The intracellular proteolytic processing of HAstV-8 VP90 to generate VP70, the protein that forms the mature particle, occurs at its carboxy terminus and has been previously related with the release of the virus from the cell (Mendez et al., 2004). To find out whether that correlation indeed exists, a time-course analysis along infection was carried out. Cells were infected and the infectious particles, as well as the viral proteins present in the supernatant and in the cell fraction, were analyzed. Quantification of viral particles yielded a typical one-step growth curve, in which the amount of infectious particles started to increase after 8 h, reaching the highest titer at 12 hpi, which was maintained up to 24 h (Fig. 1A). This increase was in the intracellular as well as in the extracellular particles, although, only about 10% of the total were found extracellular (Fig. 1A). Regarding viral proteins, VP90 started to be detected at 8 hpi, and it was present up to 24 hpi, while its proteolytic product VP70 appeared in the cell fraction at 12 hpi (Fig. 1B). VP70, but not VP90, was clearly observed in the extracellular fraction at 16 hpi (Fig. 1C).

The processing of VP90 to VP70 has been associated with the activity of cellular *Casp* (Mendez et al., 2004), so that to confirm the activity of executioner *Casp*, the cleavage of PARP, considered as classical substrate of these proteases (Germain et al., 1999; Tewari et al., 1995), was followed in this experiment. As observed in Fig. 1D, the 85 kDa *Casp*-dependent cleavage product of PARP appeared at 12 hpi, in coincidence with the cleavage of VP90. The same product was observed in TRAIL-treated uninfected cells, used as control for *Casp* activation (Strater et al., 2002). The *Casp*-dependent cleavage of PARP requires a productive astrovirus infection since its inactivation with psoralen-UV, treatment that reduces drastically its infectivity,

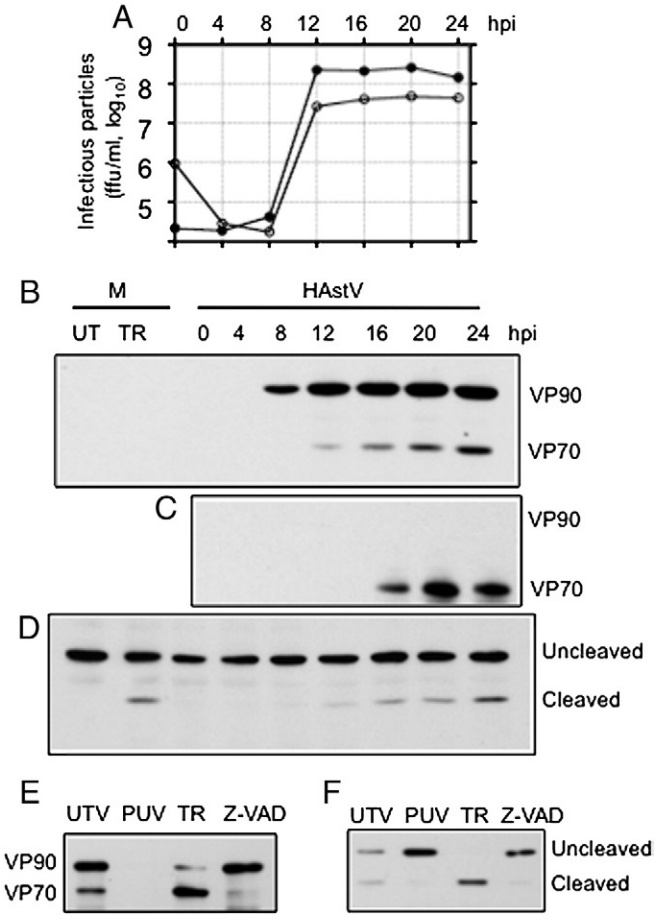

Fig. 1. Processing of the HAstV structural protein VP90 coincides in time with the proteolytic cleavage of PARP, which depends on astrovirus replication. Caco-2 cells were infected with HAstV at moi of 10, and at different time points (from 0 to 24 hpi), the extracellular and cell-associated fractions were analyzed for infectious viral particles and protein content. (A) Particles in the extracellular (empty circles) and in the cell-associated (filled circles) fractions were quantified after trypsin treatment. Cell-associated (B and D) and extracellular (C) proteins were analyzed by Western blot, using anti-HAstV (B and C) and anti-PARP (D) as primary antibodies, as indicated. (E and F) Caco-2 cells were infected with trypsinized virus untreated (UTV) or treated with psoralen-UV (PUV) and the viral proteins (E) and PARP (F) were analyzed at 20 hpi. Proteins from infected cells with untreated virus maintained in the presence TRAIL (TR) and Z-VAD.fmk (Z-VAD) were also analyzed, to confirm caspase-dependent cleavages. M, mock-infected cells; HAstV, astrovirus infected cells; UT, untreated; and TR, TRAIL-treated cells. Results shown are representative of three independent experiments made in duplicates.

although not by affecting the virion structure (Groene and Shaw, 1992) did not induce it, as observed in Fig. 1E and F.

Thus, executioner *Casp* indeed seem to be active upon astrovirus infection and their activity coincides in time with the cleavage of VP90; however, it was unknown whether initiator *Casp* were activated at earlier times of infection.

General Casp activation occurs upon HAstV infection

To determine the activation of specific *Casp*, as well as the time at which that occurs, infected cells were analyzed at different time points. *Casp* activity was followed by the cleavage of peptides preferentially recognized by every protease, coupled to aminoluciferin and *p*-nitroaniline. Substrates included DEVD-, LETD-, and LEHD-aminoluciferin, preferential substrates for *Casp-3/7* (Garcia-Calvo et al., 1999), *Casp-8* (Thornberry et al., 2000) and *Casp-9* (Thornberry et al., 1997) and LEVD-*p*-nitroaniline, preferential substrate for *Casp-4* (Talanian et al., 1997), respectively. Cell treatment with TRAIL, staurosporine, and tunicamycin, used as controls (Hitomi et al., 2004a; Stepczynska et al., 2001; Suliman et al., 2001), showed that activation of *Casp-3/7*, *-8*, *-9*, and *-4*, respectively, could be detected by this assay (Fig. 2, panels A to D). Thus, under control conditions, *Casp's* activity was clearly detected at 6 h and it was maintained high up to 24 h post-treatment. Regarding peptide LEVD-*p*-NA, substrate for *Casp-4*, there was a small but significant cleaving increase at 12 h of tunicamycin treatment, indicating activation of this *Casp*. On the other hand, cleavage of these substrates by HAstV-infected cell extracts was clearly observed at 12 hpi, indicating that *Casp-3/7*, *-8*, *-9*, and *-4* had been activated at that time. *Casp* activity was maintained up to 24 hpi (Fig. 2A to C), except for the transient activity responsible for cleaving peptide LEVD (Fig. 2D).

Cleavage of *Casp* substrates can be promiscuous since more than one activated *Casp* could cleave the same motif (McStay et al., 2008); therefore, disappearance of the pro-form of every *Casp* (*pCasp*) was later studied to confirm their activation. Pro-forms of *Casp-3*, *-7*, *-8*, and *-9* were reduced in cells infected with HAstV, as well as after TRAIL treatments, indicating that more than a single *Casp* seemed to be activated upon HAstV infection (Fig. 2E). On the other hand, cleavage of pCasp-4 was undetected in HAstV-innfected cells or even upon tunicamaycin, tapsigargin (not shown), and staurosporine treatment, which induced all the rest *pCasp* cleavages, except *Casp-9* (Fig. 2E). Bid was also observed proteolytically processed during infection (Fig. 2E) (see discussion below). These results did not suggest which *Casp* could be involved in the processing of VP90, especially because all of them were active at the same time, when VP90 starts to be processed.

Several Casp are involved in the processing of VP90 to yield VP70

To investigate whether the processing of VP90 was due to a specific *Casp*, experiments to individually knock-down initiator (*Casp-4*, *-8*, and *-9*) and executioner (*Casp-3*) *Casp* were carried out. The efficiency and specificity of silencing were evaluated by determining the absence of the corresponding *pCasp*. In every case, analysis included comparison with cells that were transfected with an irrelevant siRNA, targeting Luciferase (siRNA-Luc). As shown in Fig. 3, the silencing of a given *Casp* was efficient and specific in the absence of any apoptotic stimulus, since only the silenced *pCasp* was reduced to 2–4%. The only exception was a threefold increase of *pCasp-8*, and a reduction of *Casp-3* after silencing of *Casp-4*; however, this did not correlate with modifications of *Casp-3* activity (Fig. 4E); therefore, these observations were unclear.

To confirm that *pCasp* reduction was not due to a cleavage because their activation, but due to their silencing in HAstV-infected cells, the activated-forms (*Casp**, Fig. 4A and B), or the reduction in the activity (*Casp-4* in Fig. 4C and *Casp-3* in Fig 4D), were also evaluated. Silencing of initiator *Casp-8* and *-9* was efficient in these cells since both *pCasp* and *Casp** were drastically reduced after transfection with the corresponding siRNA (Figs. 3 and 4). Although a small amount of these *pCasp* was still observed in mock-treated cells after transfection with those siRNA, these were not present after infection, indicating that HAstV induced their cleavage, and therefore, a residual protease activity existed in the knocked-down cells. A small reduction of *pCasp-8 and pCasp-9* was also observed after infection of cells transfected with the control siRNA-Luc, confirming that astrovirus infection indeed induces their activation. The same was observed after treatment

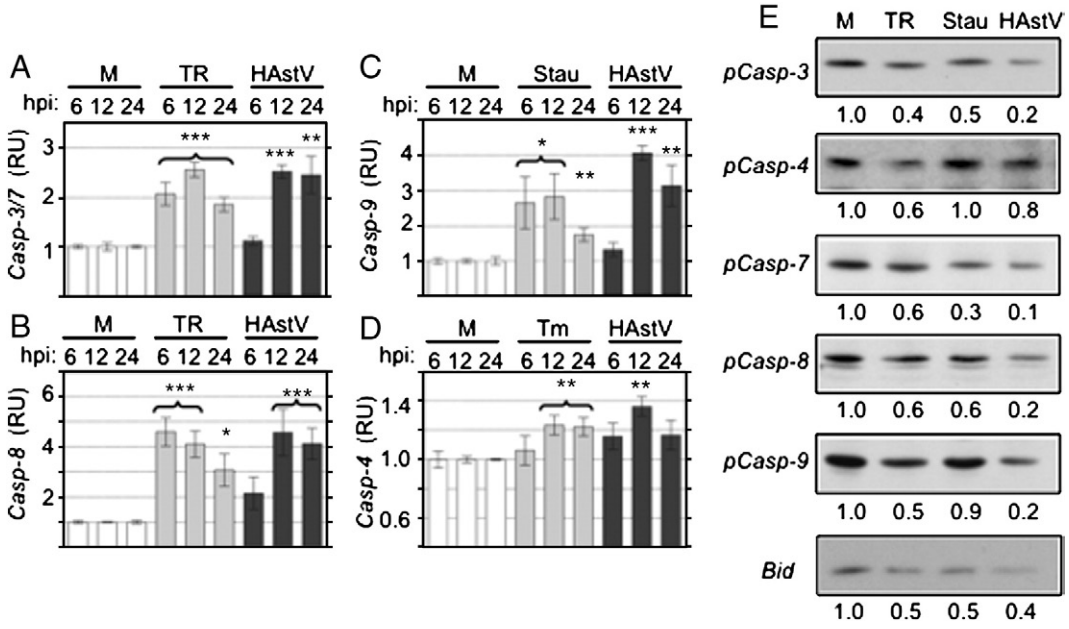

Fig. 2. *Casp* activity in cells infected with HAstV. Caco-2 cells were infected with HAstV (HAstV) at moi of 10, mock-infected (M), or treated with either TRAIL (TR), Staurosporine (Stau) or Tunicamycin (Tm). At the indicated time points (hpi), cells were harvested to determine the activity of individual *Casp* (shown in panels A to D), as well as the respective pro-enzymes and *Bid* (*pCasp* and *Bid*, panel E) by immunoblot. Relative units (RU) were calculated based on the activity in mock-treated cells. Graphs represent results of three independent experiments made in duplicates. The statistical significance indicate $^{*}P<0.01$, $^{**}P<0.001$ and $^{***}P<0.0001$. Numbers below the blots in panel E represent the relative amount of every *pCasp* detected by densitometry, taking alpha-tubulin, and mock-infected cells as the reference. Representative results of five independent experiments are shown.

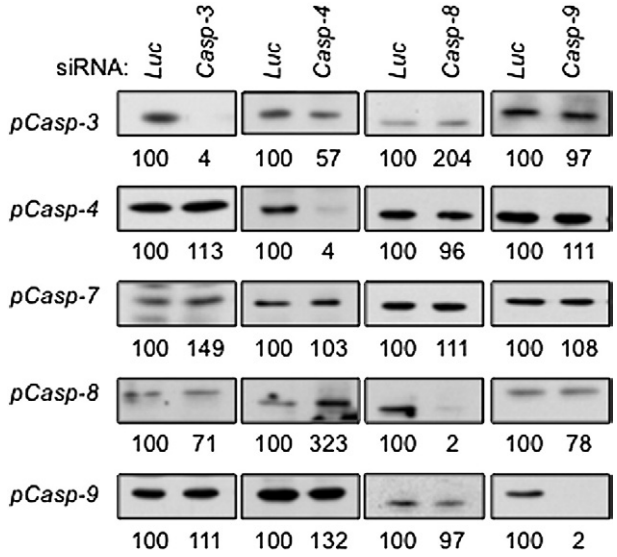

Fig. 3. Silencing of individual *Casp* in siRNA-transfected cells. Caco-2 cells were transfected with the indicated siRNA 3 days before harvesting to detect the indicated *pro-Casp* by immunoblot with specific antibodies. Every gel was also immunoblotted with antibodies to alpha-tubulin, whose signal was used as loading control. Numbers below every well indicate results of the densitometric analysis of the signal obtained by individual anti-*Casp*, based on the signal obtained with anti-tubulin. Results are representative of two to three independent experiments.

with the pro-apoptotic agents TRAIL and staurosporine, respectively, although with this at a minor extent (Fig. 4A and B). *pCasp-4* was also efficiently reduced after transfection with the specific siRNA (siRNA-C4) (Fig. 5C). Although reduction of this pro-enzyme was not obvious after infection or tunicamycin treatment in siRNA-Luc-transfected cells, the cleavage of peptide LEVD-*p*-nitroaniline increased slightly, indicating that activation of *Casp-4* occurred in both conditions. Cleavage of LEVD-*p*-nitroaniline was reduced to basal level after transfection with siRNA-C4, indicating that silencing with this siRNA was efficient and that this protease was activated in HAstV-infected cells (Fig. 4C). As shown above, the executioner p*Casp-3* was drastically reduced in control cells transfected with the homologue siRNA-C3, compared with cells transfected with siRNA-Luc, and it was no longer detected in TRAIL-treated and HAstV-infected cells, after silencing (Fig. 4D); its activity was also reduced by silencing (Fig. 4E, see below).

Although Casp silencing was specific based on individual *pCasp* cleavages (Fig. 3), given that *Casp* activation occurs in a cascade manner (Kang et al., 1999), it was still possible that blocking expression of a single *Casp* could affect indirectly the activation of downstream executioner *Casp* in HAstV-infected cells. To clear this, *Casp-3/7* activity was evaluated in cells transfected with every single siRNA-C4, siRNA-C8, or siRNA-C9 and then infected with HAstV or treated with the pro-apoptotic agents, as controls. As observed in Fig. 4E, the activity of *Casp-3/7* was reduced in HAstV-infected cells that were previously transfected with individual siRNA targeting *Casp-8* or *-9*, compared with those transfected with the irrelevant siRNA. This observation suggested that these initiator *Casp* could modulate the activity of executioner *Casp* in cells infected with astrovirus. Cells transfected with siRNA-C8 and treated with TRAIL showed a lower activity of *Casp-3/7*, as expected (Fig. 4E). Surprisingly, knocking-down *Casp-9* did not affect the activity of the executioner *Casp3/7* in staurosporine-treated cells. On the other hand, blocking *Casp-4* expression had no effect on *Casp-3* activity in HAstV-infected or tunicamycin-treated cells (Fig. 4E). As expected, transfection of siRNA-C3 dropped *Casp-3* activity, even in mock-treated cells, confirming a basal *Casp-3* activity in Caco-2 cells (Fig. 4E). These data indicated that initiator *Casp-8* and *-9*, but not *Casp-4*, could somehow modulate the activity of the executioner *Casp-3* in HAstV-infected cells, through a still undetermined pathway.

Given that several *Casp* were activated and that the carboxy-end of VP90 that is cleaved includes motifs that could be recognized by more than one of these proteases (Mendez et al., 2004), it was unclear which one of them could be actually responsible for that processing. Thus, for a better understanding of the role of these enzymes on VP90 processing, this was evaluated in cells that were knocked-down for every single *Casp*. As shown in Fig. 5, the proteolytic processing of VP90 to VP70 was reduced (between 48% and 62%) in cells knocked-down for *Casp-3*, *-4*, or *-9*, but not in cells knocked-down for *Casp-8* (Fig. 5A). Unexpectedly, *Casp-3/Casp-9* co-silencing block VP90 processing at the same level than individual silencing (Fig 5A), suggesting that additional *Casp* participated in that cleavage. Reduction in the processing did not directly correlate with the level at which proteases expression was blocked (more than 95%, Fig. 3). This finding could be due to the small fraction of protease synthesized and activated upon silencing was enough to cleave VP90 or due to an indirect effect, in which such small amount of active enzyme was able to cleave and activate the *Casp* actually responsible. Alternatively, more than one *Casp* could be directly involved in the processing of the structural protein. To distinguish among these possibilities, VP90 was *in vitro* translated and treated with purified active proteases, independently (Fig. 5B). Every *Casp* used in this experiment was active since they were able to cleave their respective substrates coupled to aminoluciferine and *p*-NA (not shown) and to cleave *in vitro* translated *Casp-3* dominant negative mutant (DN-C3); as expected, *Casp-3* cleaved DN-C3 at a minor extent (Fig. 5E). Treatment of VP90 with purified *Casp-3*, *-8*, and *-9* yielded a protein of 70 kDa (Fig. 5B) similar in size to VP70 produced in HAstV-infected cells (Fig. 5C); *Casp-4* yielded a small amount of the same VP70 product. The 70-kDa protein was not observed when digestion was carried out in the presence of Z-VAD.fmk, indicating that cleavages were *Casp*-dependent (Fig. 5D). These results indicate that *Casp-3*, *-9*, and *-8*, whose silencing did not block the processing in cells (Fig. 5A), can recognize VP90 as substrate to cleave it, likely at the same site, to yield VP70. Thus, although VP90 can be substrate of *Casp*, only some of them could recognize it and contribute for its cleavage during infection.

To elucidate the cleavage site on VP90 that yield VP70, truncated VP90 mutants that end at $DEVD_{686}$, $EETD_{672}$, $EPET_{654}$, and TY_{655}kvr (Fig. 6) were produced and compared with the product obtained by digestion of VP90 with *Casp-3*. These sites were selected to produce the truncated mutants because motifs $DEVD_{686}$, $EETD_{672}$, and $TYVD_{657}$ were predicted as cleaved to yield products of around 70 kDa. As shown in Fig 6B, proteins VP-$DEVD_{686}$ and VP- $EETD_{672}$ were larger than the product observed after digestion of VP90 with *Casp-3*. On the other hand, given that motifs potentially recognized by *Casp* are not present upstream $TYVD_{657}$ and that proteins VP-$EPET_{654}$ and VP- TY_{655}kvr migrated similarly to VP70, the motif $TYVD_{657}$ was the most likely to be cleaved to yield VP70.

Executioner Casp activity may be involved in the release of astrovirus through a non-lytic mechanism

Previous observations suggested that the release of astrovirus was independent of cell death, although directly related with the processing of VP90 (Mendez et al., 2004). Since in this work a general *Casp* activation was observed, it was still possible that cell death would be involved in that step of the replication cycle. To discriminate this possibility, the integrity of infected cells membrane was determined by LDH leakage and by trypan blue staining. Release of LDH was unaffected during HAstV infection, compared to mock-infected cells, even when infection was at high moi and maintained up to 48 hpi (Fig. 7A). This was also observed in cells transfected with every siRNA (Fig. 7B), indicating that this procedure did not affect cell membrane. No differences were found among cells when their viability was quantified by trypan blue staining, where less than 1% of cells infected at high moi

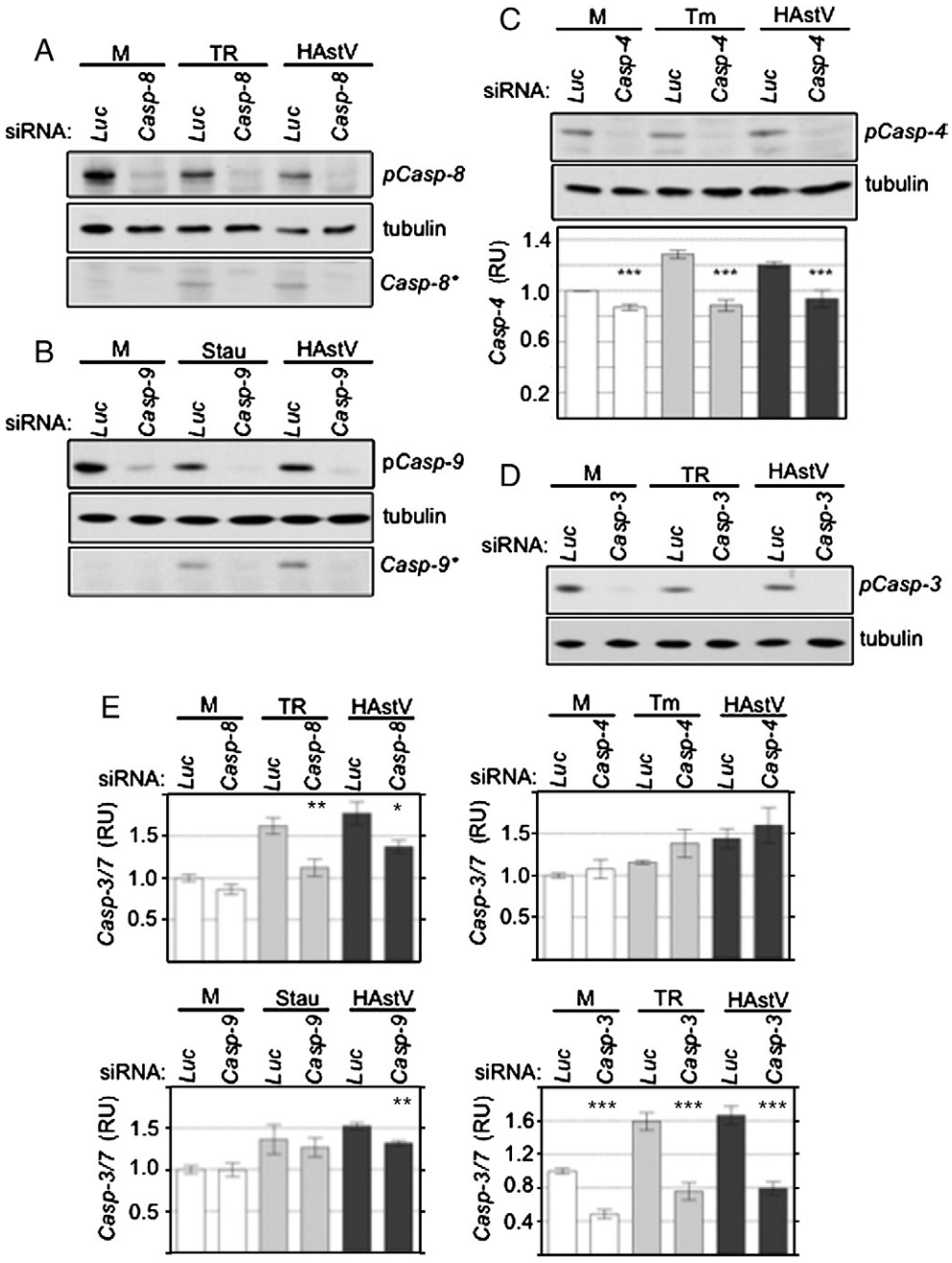

Fig. 4. Silencing of individual *Casp* in HAstV-infected cells and its effect on executioner Casp activity. Caco-2 cells were transfected with the indicated siRNA 3 days before either HAstV infection at moi of 10, or treatment with the indicated drug. After 20 hpi, cells were harvested for immunoblot with antibodies to *Casp-8* (panel A), *Casp-9* (panel B), *Casp-4* (panel C), and *Casp-3* (panel D), including the complete (*pCasp*) and, for *Casp-8* and *Casp-9*, the active forms (*Casp**); anti-alpha-tubulin was used as loading control. For *Casp-4* (panel C), the activity, instead of the active form, was measured. Cells were also independently harvested at 20 hpi for *Casp-3* activity measurements. Relative units (RU) were calculated similarly to how it was mentioned in Fig. 2. Abbreviations are the same as in Figs. 2 and 3. Average and standard deviation of three independent experiments, made in duplicates, are shown. $^{*}P<0.01$, $^{**}P<0.001$, $^{***}P<0.0001$. Average of three independent experiments assayed in duplicate are shown. $^{***}P<0.0001$.

was stained (not shown). These data confirmed that cell membrane disruption is not necessary for the virus to be released; however, it was unclear whether it was dependent on VP90 proteolytic processing, as previously suggested (Mendez et al., 2004). To elucidate any relationship between these two events of the replication cycle, virus release was evaluated in cells where VP90 processing was blocked *due to Casp* silencing (Fig. 7A). As observed in Fig. 7C, reduction in virus release was more pronounced after *Casp-3* silencing, to less than 60%; knocking-down *Casp-4* and *Casp-9* had a slight effect, if any; while *Casp-8* silencing had no effect. Contrary to previous suggestions (Mendez et al., 2004), these data showed no correlation between virus release and VP90 processing, but they did with *Casp-3* activity. Thereafter, virus release was determined by incubating infected cells with *Casp* inhibitors, including Ac-DEVD-CHO, a potent inhibitor for executioner Casp-3/7, and Ac-LEHD-CHO and Ac-IETD-CHO, which have been considered inhibitors for *Casp-9* and *Casp-8*, respectively (Fig. 7D). In the presence of Ac-DEVD-CHO, the release of the virus was blocked at similar levels than those observed after infection in the presence of the pan-*Casp* inhibitor Z-VAD.fmk, while inhibitors for the initiator *Casp* had no effect. On the contrary, TRAIL treatment increased the exit of the virus from the cell, as previously reported (Mendez et al., 2004). Thus, executioner Casp seems to be the most involved in the release of the virus from the cell through a mechanism that does not involve cell lysis, but other Casp could participate in VP90 processing.

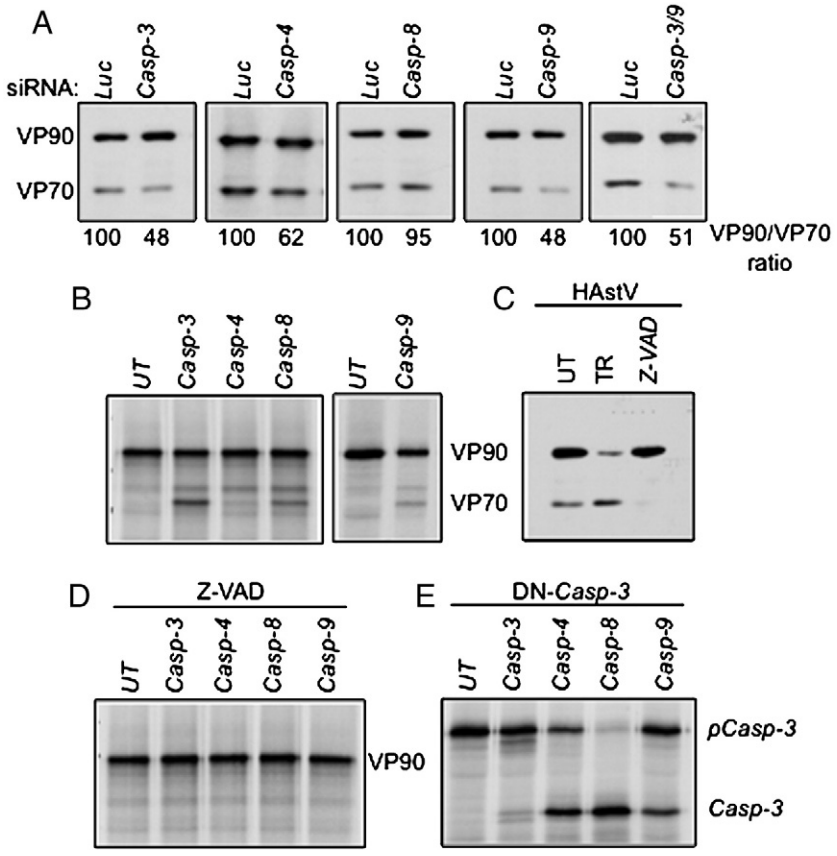

Fig. 5. VP90 is substrate for initiator and executioner *Casp*. In panel A, Caco-2 cells were transfected with the indicated individual siRNA or co-silencing *Casp-3* and *Casp-9* (*Casp-3/9*) and infected with HAstV, as described in Fig. 3. Viral proteins were detected by immunoblot with anti-HAstV, and the ratio VP90/VP70 was calculated based on densitometry. Proteins VP90 (panels B and D) and DN-*Casp-3* (panel E) were *in vitro* translated, in the presence of Express-[^{35}S]-Met labeling mix, and either untreated (UT) or digested with the indicated active enzyme. The same reaction mixtures that included VP90 were incubated in the presence of Z-VAD.fmk (panel D) to confirm *Casp*-dependent cleavages. Proteins (panels B, D, and E) were detected by autoradiography after electrophoresed. Proteins of HAstV-infected cells (HAstV, panel C) untreated (UT) or treated either with TRAIL (TR) or Z-VAD.fmk were analyzed by immunoblot with anti-HAstV to compare the proteins obtained by *in vitro* translation. Viral proteins and the products of *Casp*-digestion are indicated.

Discussion

Features indicative of apoptosis have been observed in Caco-2 cells infected with two HAstV strains of different serotypes (Guix et al., 2004a; Mendez et al., 2004). In the case of HAstV-8, *Casp* activity correlated with the processing of the ORF2 primary product, VP90, at its carboxy terminus to generate the protein VP70 that forms the mature extracellular virion. This processing was blocked by the pan-*Casp* inhibitor Z-VAD.fmk (Mendez et al., 2004). Such activity was also associated with the presence of viral particles in the extracellular fraction of infected cells (Mendez et al., 2004), although not with the yield of virus progeny because the pan-*Casp* inhibitor does not block particles formation (Mendez et al., 2004, 2007). To explore the role of individual *Casp* on VP90 processing and virus release, activation of specific *Casp*, as well as these two events, was determined in cells that were knocked-down by siRNA molecules. *Casp-8*, but not *Casp-9*, was suggested as the main initiator *Casp* activated upon astrovirus infection in previous reports (Guix et al., 2004a); however, in this work, cleavage of initiator and executioner *pCasp*, as well as their activity, was detected and continued up to 24 hpi. This observation impeded to suggest the pathway by which *Casp* were initially activated during HAstV infection. As mentioned above, experiments with HAstV-4 suggested that *Casp-8* activate the extrinsic pathway (Guix et al., 2004a). Cleavage of Bid observed in this work (Fig. 3) agrees with this assumption; however, results shown here would indicate that more than one pathway (and stimuli?) would be probably involved in triggering Casp activation, since initiator and executioner *Casp* activation coincided in time. In addition, executioner *Casp-3/7* activity was reduced, although not to basal levels, after silencing both initiator Casp-8 and Casp-9, independently. In principle, the cleavage of Bid observed in HAstV-infected cells (Fig. 3) would suggest *Casp-8* as the initiator; however, in *Casp-8*-silenced infected cells, although *Casp-3* activity was reduced, Casp-dependent cleavages still occurred, such as VP90 (Fig. 5A) and Bid cleavages (not shown), indicating the activation of *Casp* in a *Casp-8*-independent manner in HastV-infected cells although it cannot be discarded that other proteases could mediate Bid cleavage in these conditions, as reported (Yin, 2006). On the other hand, the *Casp*-dependent cleavage of VP90 was still observed upon *Casp-3*/*Casp-9* co-silencing, indicating that a *Casp* activity was present and could be triggered in the absence of either *Casp-8* or *Casp-9*, and therefore, suggesting that more than one pathways may be involved in the activation of *Casp* activity during infection. *Casp* activation seems to be triggered in a post-virus binding/entry step and probably requires virus translation and/or replication, since particles inactivated by psoralen-UV, which seems not to affect the structure of the virus and, therefore, the early steps of infection, as reported for rotavirus (Groene and Shaw, 1992), were not able to induce such activation. Whether nsp1a, as suggested previously (Guix et al., 2004a), or additional factors, triggers *Casp* activation remains to be determined. Limited studies on the cell response to HAstV infection exist, which could give a clue on the mechanism involved in *Casp* activation. Recently, extracellular signal-regulated kinases (ERK-1 and ERK-2) were found active at early stages of astrovirus infection (Moser and Schultz-Cherry, 2008). Given that these molecules may participate in triggering apoptosis by phosphorylating pro-apoptotic factors in some

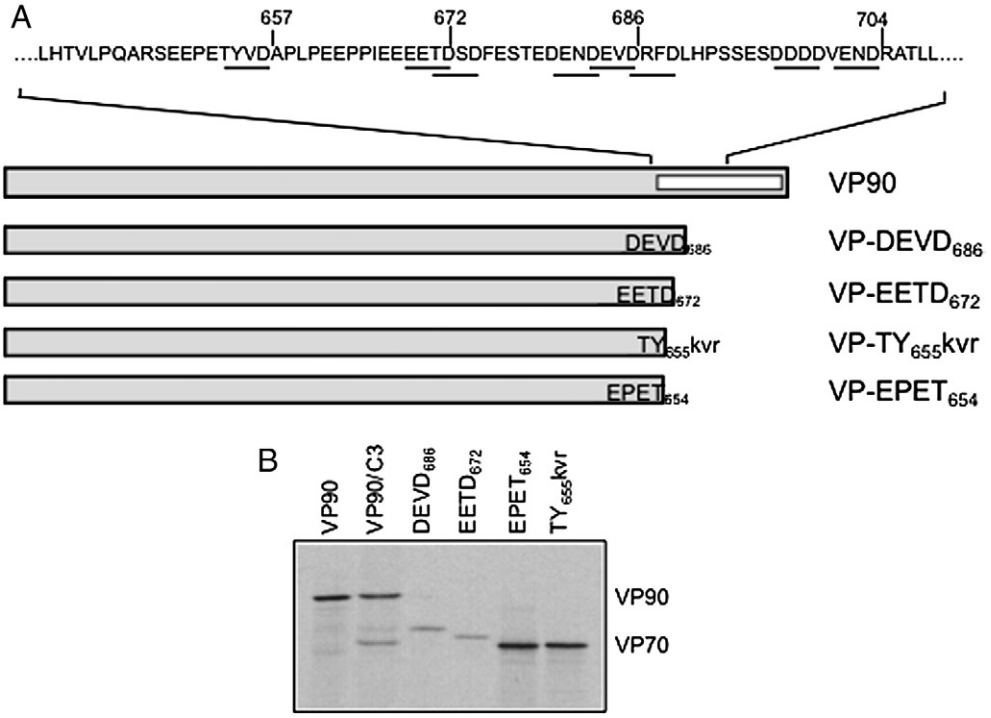

Fig. 6. Processing of VP90 at motif $TYVD_{657}$ yields VP70. (A) Partial sequence, in which *Casp*-recognition motifs are underlined, and scheme of the truncated proteins produced are shown. Proteins are named based on the sequence and the amino acid residue in which they end, as indicated. Minor letters in TY_{655}kvr indicate residues included in the construct that are not part of the HAstV-8 structural protein. Numbers above the sequence indicate the amino acid residues, based on HAstV-8 sequence, while the white box, the Asp-rich region in VP90. (B) Proteins were *in vitro* translated and analyzed by autoradiography, as in Fig. 5. Proteins VP90 and VP90 treated with CAsp-3 (VP90/C3) were used as reference of the viral proteins migration (as indicated).

cells (Mebratu and Tesfaigzi, 2009), they could participate in the activation of *Casp* during HAstV infection; however, this hypothesis requires further investigation.

The processing of VP90 to yield VP70 is blocked by the pan-*Casp* inhibitor Z-VAD.fmk and promoted by TRAIL (Mendez et al., 2004), suggesting a role of *Casp* on this cleavage in HAstV-infected cells. In this work, it was confirmed that indeed *Casp-3* and *-9*, but not *Casp-8*, were involved in VP90 processing, since this was partially blocked by individually knocking-down those proteases. However, these proteases in its active form, including *Casp-8*, were able to cleave the protein in an *in vitro* assay, indicating their potential to recognize VP90 as substrate in infected cells. Casp-4, on the other hand, seems to contribute to VP90 processing in infected cells, since this was slightly reduced upon silencing; however, its role on this event remains unclear since it barely cleaved *in vitro* translated VP90. Hence, the processing of VP90 observed in infected cells could be carried out in a complex manner, in which more than one *Casp*, either directly or indirectly, could participate. An indirect effect was appreciated in the case of knocking-down *Casp-9*, which affected negatively the activity of *Casp-3*; however, VP90 processing was unaffected by *Casp-8* silencing that also reduces *Casp-3* activity. Thus, more than one factor seems to be involved in this event, since silencing of individual *Casp*, independently, or even *Casp-3/9* co-silencing, both of which participate in that cleavage (Fig. 5), did not block completely the processing of VP90, but it was mostly blocked in the presence of the pan-*Casp* inhibitor Z-VAD.fmk. Additional factors, such as the cellular localization of VP90 and of the proteases and interaction of these proteins with cell factors, could contribute to that processing, as it has been described for other *Casp* substrates (Ramuz et al., 2003). Regarding cell localization, VP90 has been found in at least two different cell compartments, in one of which, when associated with membranes, was protected from proteases digestion, especially at its carboxy-terminus (Mendez et al., 2007), where the *Casp* recognition motifs are located (Mendez et al., 2004, 2007). During infection, VP90 is cleaved at different sites in the carboxy-end region to yield intermediates of 75–82 kDa and the more abundant product of cleavage in the cell, VP70 (Mendez et al., 2004). *In vitro*, the *Casp*-dependent proteolysis of VP90 seems to occur similarly, independently of the *Casp* tested, since the putative carboxy-terminal product of 20 kDa was not observed (data not shown). The structural protein contains an Asp-rich region containing *Casp* recognition motifs that are highly conserved among all astroviruses (Mendez et al., 2004). In the particular case of HAstV-8 VP90, several motifs (underlined in Fig. 6) including $VEND_{704}$, $DEVD_{686}$, $EETD_{672}$, and $TYVD_{657}$ were predicted to be cleaved (analysis made by GraBCas software) (Backes et al., 2005). To determine which one of them could be the cleavage site to yield VP70, truncated mutant proteins were produced and analyzed. Although EETD and DEVD are the most conserved among all astroviruses, motif $TYVD_{657}$, was mapped in HAstV-8, since proteins that end at residues 654 and 655 gave the size than that of VP70. Thus, $VEND_{704}$, $EETD_{672}$, and $DEVD_{686}$ may be cleaved to yield the intermediates of 75–82 kDa observed upon infection (Mendez et al., 2004). It remains to be determined the role that those cleavages have on astrovirus biology.

As with VP90 processing, the release of HAstV from the cell is affected similarly with Z-VAD.fmk and TRAIL (Mendez et al., 2004). Accordingly, in this work, virus exits from the cell coincided with general *Casp* activity at 12 hpi. However, in contrast to that observed for VP90 processing, virus release was differentially affected after silencing individual *Casp*, being most affected after transfection with siRNA against *Casp-3*. The role of *Casp-3* on virus release was confirmed by infecting Caco-2 in the presence of peptide inhibitors Ac.DEVD-CHO, Ac-LEHD-CHO, and Ac-IETD-CHO. Ac.DEVD-CHO, specific for executioner *Casp3/7*, was the only one able to block the release of astrovirus, at similar extent as the pan-*Casp* inhibitor Z-VAD.fmk did, suggesting that executioner *Casp-3* (and probably *Casp-7*) is necessary for that event of the replication cycle. In contrast, silencing of *Casp-9* induces a slight reduction of virus release (approximately 10%), probably through an indirect effect on Casp-3 as it has been observed in this work and reported elsewhere (Slee et al., 1999; Yukioka et al., 2008), despite that

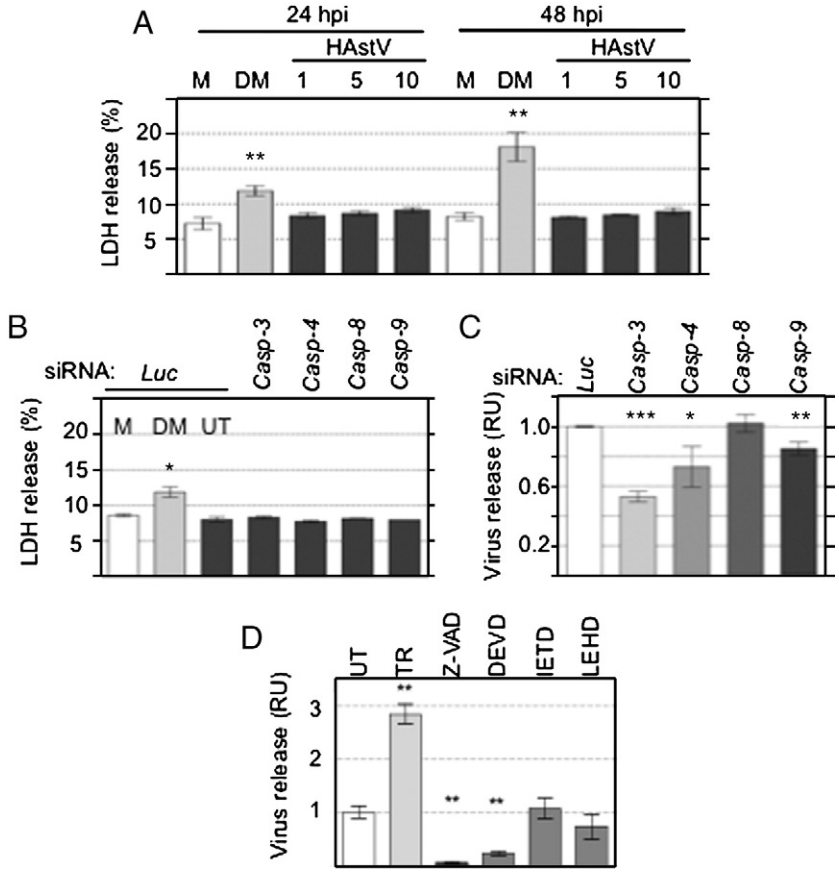

Fig. 7. Executioner *Casp* favors astrovirus release by a non-lytic mechanism. Cells were infected with HAstV at the indicated moi (1 to 10) and harvested at 24 and 48 hpi (including DMSO treatment as positive control), and the release of LDH was calculated as percentage of the total (panel A). Caco-2 cells were transfected with the indicated siRNA and infected with HAstV (panels B and C), as indicated in Fig. 2. Extracellular and intracellular LDH activity (panel B) and infectious particles (panel C) were quantified at 20 hpi and expressed as percentage of the total LDH, and as the ratio of particles found in extracellular/intracellular fractions, compared to that observed in cells transfected with the siRNA-Luc, respectively. Virus release was also measured from cells infected with HAstV at moi of 10 and incubated for 20 h with MEM alone (UT-untreated), or MEM containing TRAIL (TR), Z-VAD.fmk (Z-VAD), or the peptide inhibitors Ac-DEVD-CHO (DEVD), Ac-LEHD-CHO (LEHD) and Ac-IETD-CHO (IETD). M, mock-treated cells; DM, DMSO treatment; UT, untreated cells. Graphs represent the average of at least three independent experiments made in duplicates. $^{*}P<0.01$, $^{**}P<0.001$.

it blocked VP90 processing at the same extent as *Casp-3* silencing. As mentioned above, the role of Casp-4 on VP90 processing and virus release was unclear since the effect after its silencing, and its activation during infection, although consistent, was weak. Thus, the processing of VP90 and the release of the virus seem to be two *Casp*-related but independent events, so that viral particles containing VP70, once VP90-containing particles have been processed by *Casp-3*, *-9*, or any other unidentified *Casp*, would be able to exit the cell, but only in the presence of *Casp-3* activity (or other executioner *Casp*, like *Casp-7*). Executioner *Casp* are mainly responsible for the biochemical and morphological changes in apoptosis leading to cell death (Slee et al., 2001); therefore, the release of the virus could be due to an increase of this death. In fact, cellular proteins such as lamin A and PARP and defects in the mitochondrial integrity have been observed upon astrovirus infection (Mendez et al., 2004). However, based on this work and that of others (Moser et al., 2007), HAstV infection does not enhance disruption of cell membrane, as judged by LDH release, up to 36–48 hpi, even in cells infected at high moi. A low percentage of infected cells showed to be TUNEL-positive cells at 24 hpi (Guix et al., 2004a; Mendez et al., 2004), time at which VP90 processing and virus release had occurred, indicating that at this time, most of the cells were viable. Thus, cell viability seems not to be drastically affected in HAstV-infected cells and therefore does not seem to be necessary for virus release. Previous reports indicate that astrovirus release was blocked when HAstV-infected cells were treated with Z-VAD.fmk after being treated with TRAIL, conditions in which VP70 was the structural protein more abundant (Mendez et al., 2004), and that frequently increases death, either by necrosis or autophagy, in many cell lines (Vandenabeele et al., 2006). Thus, HAstV release seems to require both *Casp* activity and VP90 cleavage, but not cell lysis.

How can astrovirus be released in the absence of cell lysis but with active executioner *Casp*? Cell lysis due to secondary necrosis is observed at late stages of apoptosis, especially when apoptotic cells are not phagocytosed (Silva et al., 2008). At early times, the apoptotic cell is not lysed but its membrane blebs to generate apoptotic bodies, which are usually phagocytosed by other cells. Secondary necrosis does not seem necessary either for astrovirus release since cell lysis was not detected at up to 48 hpi and virus release started at 12 hpi. On the other hand, apoptotic bodies have been suggested as vehicles for chicken anemia virus release (Teodoro and Branton, 1997) because virus particles have been found in these structures. Attempts to detect these structures in Caco-2 cells infected with HAstV have failed so far (data not shown); therefore, it remains to be determined whether this kind of cell structure is important for virus release.

It is important to mention that *Casp* activation does not always result in cell death and secondary necrosis. The extent at what these enzymes are activated (Kuranaga and Miura, 2007) and the cell proteins that interact with them, such as alpha-fetoprotein (AFT) (Li et al., 2009), can modulate cell death progression. In this work, every *Casp* tested was not completely processed to yield the activated form in infected cells, and therefore, their activity did not increase dramatically, even with TRAIL and staurosporine treatments,

independently, suggesting that levels of *Casp* activation and consequently cell death were low in these cells. Previous reports have associated executioner *Casp* activity with intracellular transport of viral proteins. For example, *Casp-3* activity is necessary for the intracellular transport of influenza virus protein NP (Wurzer et al., 2003); in addition, a DEVDase *Casp* activity, encoded by *Spodoptera frugiperda* ascovirus, participates in the release of this virus, favoring the formation of vesicles that contain viral particles, which are necessary for virus dispersion (Bideshi et al., 2005). On the other hand, Casp-3 activation has correlated with the cleavage of proteins that are necessary for transport among different organelles, such as giantin and syntaxin-5 (Lowe et al., 2004), and proteins involved in endocytosis (Austin et al., 2006). Although the specific role of executioner *Casp* on astrovirus release remains to be determined, it is possible that the executioner *Casp* could participate in, or interfere with, the intracellular traffic of viral particles that contain VP70, but not VP90, in their way to the cell exterior.

Until recently, it was considered that non-enveloped viruses, such as astroviruses, were released from the cell due to cell membrane destabilization. This has been demonstrated with virus such as Coxsackie (van Kuppeveld et al., 1997); however, observations with poliovirus suggest that naked viruses could exit the cell through a non-lytic mechanism, probably involving autophagic vesicles (Jackson et al., 2005). In the case of HAstV, it is unknown whether autophagy is induced during infection, although double membrane vesicles, a hallmark of this process (Deretic and Levine, 2009), containing astrovirus particles have been observed in infected cells (Guix et al., 2004b). Further experiments are necessary to determine whether autophagy is induced during HAstV infection and whether it plays a role on virus release.

Data of this work suggest that the release of the virus is carried out through a non-lytic mechanism that depends, at least, on two related events: the processing of VP90 at the motif $TYVD_{657}$ to generate particles formed by VP70 and the activity of executioner *Casp*.

Materials and methods

Virus and cells

Cells from a human colon adenocarcinoma (Caco-2) obtained from the American Type Culture Collection (ATCC) were used in this work. Cells were cultivated for 3–4 days in Dulbecco modified essential medium (DMEM) (Sigma Cat. D7777), supplemented with non-essential amino acids (Gibco Cat. 11140) and 10% fetal bovine serum (FBS) (Cansera) at 37 °C and 10% CO_2. Cells were non-differentiated under these conditions. Viral stocks of HAstV (strain Yuc8, passages 28–31) were prepared as previously described (Mendez et al., 2002), using 0.5 as the multiplicity of infection (moi), and activating the virus with trypsin (200 μg/ml, Gibco Cat. 27250-18) for 1 h at 37 °C, and adding soybean trypsin inhibitor (200 μg/ml) just before inoculation to the cells. When virus infectivity would be determined later, the excess of trypsin inhibitor was removed by washing twice the cell monolayer with MEM. Virus infectivity was quantified by immunoperoxidase staining, using anti-HAstV as primary antibodies, as previously described (Mendez et al., 2004). In experiments described below, virus infection was carried out on a confluent cell monolayer at moi of 10 with trypsin-activated virus, and harvested 20 h post-infection (hpi), unless otherwise is indicated. Inactivated virus was obtained by psoralen and UV treatment (20 μg/ml and 15 min with $UV_{360\ nm}$ light) after trypsin treatment, as previously described (Groene and Shaw, 1992). In general, virus titer diminished 4.5 logs and protein products after trypsin treatment were the same as those obtained from the native virus under these conditions; therefore, it was considered that the structure of the inactivated virus was unaffected by psoralen treatment. In every experiment, mock-infected cells were treated similarly, including the addition of trypsin and trypsin inhibitor to the inoculum.

Sera and reagents

Rabbit polyclonal serum to HAstV (Yuc8 strain) has been previously described (Mendez et al., 2004; Mendez-Toss et al., 2000). Antibodies to *Casp-8* (Cat. sc-6136), *Casp-9* (Cat. sc-17784), Casp-4 (Cat. sc-56056), and anti-BID (Cat. sc-11423) were from Santa Cruz Biotechnology; antibodies to *Casp-3* (Cat. 610322), *Casp-7* (Cat. 556541), and to the cleaved form of *Casp-8* (Cat. 556466) were from BD Biosciences Pharmingen, and antibodies to the cleaved form of *Casp-9* were from Calbiochem (Cat AP1026). Anti-Poly-ADP-ribose polymerase (PARP) (Cat. 9546) and anti-alpha-tubulin (Cat. 18-0092) were purchased to Cell Signalling and Zymed, respectively. TRAIL (Cat. SE-721), used at 4 μg/ml in this work; Z-Val-Ala-Asp-fluoromethylketone (Z-VAD-fmk, Cat. P-416) used at 50 μM, Ac-LEHD-CHO (Cat. P-446) and Ac-IETD-CHO (Cat. P-430) used both at 100 μM, and Ac-DEVD-CHO (Cat. P-414) used at 2 μM, were purchased from BIOMOL. Staurosporine (Cat. S4400) that was used at 2 μM and psoralen (Cat. P8399) were obtained from Sigma, while Tunicamycin was from Boehringer Mannheim (Cat. 724556) and used 100 μg/ml. The active proteases *Casp-3* (Cat. 235417), *Casp-8* (Cat. 218769), *Casp-9* (Cat. 218807), and *Casp-4* (Cat. 218720) were purchased from Calbiochem.

Quantification of Casp activity

Activity of *Casp-3*/*7*, *Casp-8*, and *Casp-9* was determined by measuring the cleavage of their preferential substrates DEVD, LETD and LEHD coupled to aminoluciferin, respectively, using Caspase-Glo reagents (Promega). Based on the manufacturer recommendations, mock- or infected-cells were lysed with the corresponding reagent (either Caspase-Glo-3/7, -8, and -9), and the luminescence was measured after 30 min in the Monolight 2010 apparatus (Analytical Luminescence Laboratory). On the other hand, *Casp-4* activity was determined by colorimetry, using its preferential substrate LEVD-*p*-nitroaniline (LEVD-*p*NA), according to the manufacturer instructions (Biovision Cat. 1110-200). Approximately 10^6 cells were recovered and lysed with buffer (50 mM HEPES pH 7.4, 0.1%, Chaps, 1 mM DTT, 0.1 mM EDTA, and 0.1% Triton x-100), incubating 10 min on ice; centrifuged for 1 min at 10,000×*g*, and the supernatant was 2-fold diluted with 2× *Casp* Reaction (CR) buffer (50 mM HEPES pH 7.4, 100 mM sodium chloride, 0.1% Chaps, 10 mM DTT, 1 mM EDTA, 10% glycerol) (Stennicke and Salvesen, 1997). Every reaction was carried out with equivalent protein concentration by adding 5 μl of substrate LEVD-*p*NA and incubating 2 h at 37 °C. Optical density was measured at 405 nm. For these experiments, cells were treated with TRAIL, staurosporine or tunicamycin, as controls.

In vitro translation of VP90 and cleavage by active Casp

The plasmid that expresses HAstV-8 VP90 has been previously described (Mendez et al., 2007). This construct was used to obtain VP90 truncated mutants that end at motifs $DEVD_{686}$, $EETD_{672}$, $EPET_{654}$, and TY_{655}kvr, named VP-$DEVD_{686}$, VP-$EETD_{672}$, VP-$EPET_{654}$, and VP-TY_{655}kvr, respectively. Protein VP-TY_{655}kvr includes 3 amino acid residues (KVR) at the carboxy-end, which are not present in the structural astrovirus protein. Plasmid expressing the dominant negative mutant of *Casp-3* (DN-*Casp-3*) was kindly provided by D. E. Bredesen (Buck Institute for Research in Aging, CA). Expression of these proteins was controlled by the phage T7 RNA polymerase promoter. Linearized plasmids were mixed with a Master Mix of T_NT-T7 (Promega) and 10 μCi of Express-[^{35}S]-Met labeling mix (New England Nuclear) and incubated 1 h at 30 °C. One fraction of this reaction mixture was added independently to 3 μl of active forms of *Casp-3*, *Casp-4*, *Casp-8*, or *Casp-9* and diluted up to 25 μl with CR buffer. After

Table 1
Features of siRNA molecules.

Gene	Sequence	Nucleotide	Accession	Work Concentration	Reference
Casp-8	GAUACUGUC UGAUCAUCAATdT	796-814	NM_033356	64 μM	This work
Casp-9	GCUUCGUUUCUGCGAACUAdTdT	351-369	NM_032996	32 μM	This work
Casp-3	CACAGCACCUGGUUAUUAUdTdT	690-708	NM_032991	3.2 μM	This work
Casp-4	GGACUAUAGUGUAGAUGUA	580-599	NM_001225	1.6 μM	This work
	GAGACUAUGUAAAGAAAGA	418-437			
	GAGGGAAUCUGCGGAACUG	713-732			
	UAGAGGAAGUAUUUCGGAA	1089-1108			
Luciferase	GUGCGUUGCUAGUACCAACdTdT	851.871	AB261988.1	1.6, 3.2, 6.4 μM	Montero et al. (2008)

incubation at 37 °C for 5 h, Laemmli sample loading buffer was added and the protein products were separated by SDS-PAGE and analyzed by autoradiography.

Immunoblot

Cell monolayer was washed twice with MEM at the indicated time post-infection and harvested in Laemmli Sample loading buffer, supplemented with Complete proteases inhibitor cocktail (Roche, Cat. 11697). Proteins were electrophoresed in SDS-Polyacrylamide gels and transferred to nitrocellulose membranes (Millipore Cat. HATF00010), which were blocked with 5% non-fat dried milk in Tris-buffered saline solution plus 0.1% Tween-20 (TBS-T). Primary and secondary antibodies were diluted in the same buffer and incubated either 1 h at room temperature (when anti-HAstV, anti-tubulin, and anti-PARP are used) or overnight at 4 °C (with anti-*Casp* and anti-*Bid*). Membranes were washed, and the proteins were visualized by chemiluminescence (Luminol reagent, Perkin Elmer Cat. NEL104).

Transfection of Caco-2 cells with siRNA

For every siRNA, the optimal concentration that resulted in the lowest target protein expression and highest transfection efficiency (in every experiment, higher than 95%) was determined experimentally (Table 1). Caco-2 cells were transfected using the Nucleofector device and solution T, based on the manufacturer recommendations (Amaxa Cat. VCA-1002). Cells were infected, or treated as indicated in the corresponding section, after 3 days of transfection.

Lactate dehydrogenase leakage assays

It was carried out with the *in vitro* Toxicology Assay kit (Sigma Cat. TOX-7). Briefly, media from the cell culture was removed and stored at 4 °C, while the cell monolayer was lysed with the buffer included in the kit (previously diluted 1:10 with MEM), incubating at 37 °C for 45 min. After lysis of the cell fraction, the supernatant initially recovered and one-tenth of the cell fraction were independently mixed with the assay mixture and kept 30 min at room temperature. LDH activity was determined based on the optical density and expressed as percentage of the total activity.

Statistics

Statistical analysis for every experiment was determined by a two-tailed *T*-test with confidence interval of 99%, using the GraphPad Prism 4.0 Software (GraphPad Software, Inc.).

Acknowledgments

We thank G. Aguirre-Crespo for excellent technical assistance. We also thank D. E. Bredesen for the DN-C3 plasmid. This work was partially supported by grants 44884-Q and 79574 from CONACyT, and grants IN226106 and CRP.LA/MEX03-01 from DGAPA-UNAM and ICGB-OPS-RELAB, respectively. M.R.B.L. was supported by a scholarship from CONACyT.

References

Austin, C.D., Lawrence, D.A., Peden, A.A., Varfolomeev, E.E., Totpal, K., De Maziere, A.M., Klumperman, J., Arnott, D., Pham, V., Scheller, R.H., Ashkenazi, A., 2006. Death-receptor activation halts clathrin-dependent endocytosis. Proc. Natl. Acad. Sci. U. S. A. 103 (27), 10283–10288.
Backes, C., Kuentzer, J., Lenhof, H.P., Comtesse, N., Meese, E., 2005. GraBCas: a bioinformatics tool for score-based prediction of caspase- and granzyme B-cleavage sites in protein sequences. Nucleic Acids Res. 33 (Web Server issue), W208–W213.
Barber, G.N., 2001. Host defense, viruses and apoptosis. Cell Death Differ. 8 (2), 113–126.
Baxendale, W., Mebatsion, T., 2004. The isolation and characterisation of astroviruses from chickens. Avian Pathol. 33 (3), 364–370.
Behling-Kelly, E., Schultz-Cherry, S., Koci, M., Kelley, L., Larsen, D., Brown, C., 2002. Localization of astrovirus in experimentally infected turkeys as determined by in situ hybridization. Vet. Pathol. 39 (5), 595–598.
Bertrand, R., Solary, E., O'Connor, P., Kohn, K.W., Pommier, Y., 1994. Induction of a common pathway of apoptosis by staurosporine. Exp. Cell Res. 211 (2), 314–321.
Bideshi, D.K., Tan, Y., Bigot, Y., Federici, B.A., 2005. A viral caspase contributes to modified apoptosis for virus transmission. Genes Dev. 19 (12), 1416–1421.
Deretic, V., Levine, B., 2009. Autophagy, immunity, and microbial adaptations. Cell Host Microbe 5 (6), 527–549.
Doseff, A.I., 2004. Apoptosis: the sculptor of development. Stem Cells Dev. 13 (5), 473–483.
Finkbeiner, S.R., Le, B.M., Holtz, L.R., Storch, G.A., Wang, D., 2009. Detection of newly described astrovirus MLB1 in stool samples from children. Emerg. Infect. Dis. 15 (3), 441–444.
Fischer, U., Janicke, R.U., Schulze-Osthoff, K., 2003. Many cuts to ruin: a comprehensive update of caspase substrates. Cell Death Differ. 10 (1), 76–100.
Fuentes-Prior, P., Salvesen, G.S., 2004. The protein structures that shape caspase activity, specificity, activation and inhibition. Biochem. J. 384 (Pt 2), 201–232.
Gallimore, C.I., Taylor, C., Gennery, A.R., Cant, A.J., Galloway, A., Lewis, D., Gray, J.J., 2005. Use of a heminested reverse transcriptase PCR assay for detection of astrovirus in environmental swabs from an outbreak of gastroenteritis in a pediatric primary immunodeficiency unit. J. Clin. Microbiol. 43 (8), 3890–3894.
Garcia-Calvo, M., Peterson, E.P., Rasper, D.M., Vaillancourt, J.P., Zamboni, R., Nicholson, D.W., Thornberry, N.A., 1999. Purification and catalytic properties of human caspase family members. Cell Death Differ. 6 (4), 362–369.
Geigenmuller, U., Chew, T., Ginzton, N., Matsui, S.M., 2002. Processing of nonstructural protein 1a of human astrovirus. J. Virol. 76 (4), 2003–2008.
Germain, M., Affar, E.B., D'Amours, D., Dixit, V.M., Salvesen, G.S., Poirier, G.G., 1999. Cleavage of automodified poly(ADP-ribose) polymerase during apoptosis. Evidence for involvement of caspase-7. J. Biol. Chem. 274 (40), 28379–28384.
Groene, W.S., Shaw, R.D., 1992. Psoralen preparation of antigenically intact noninfectious rotavirus particles. J. Virol. Methods 38 (1), 93–102.
Guix, S., Bosch, A., Ribes, E., Dora Martinez, L., Pinto, R.M., 2004a. Apoptosis in astrovirus-infected CaCo-2 cells. Virology 319 (2), 249–261.
Guix, S., Caballero, S., Bosch, A., Pinto, R.M., 2004b. C-terminal nsP1a protein of human astrovirus colocalizes with the endoplasmic reticulum and viral RNA. J. Virol. 78 (24), 13627–13636.
Hildeman, D., Jorgensen, T., Kappler, J., Marrack, P., 2007. Apoptosis and the homeostatic control of immune responses. Curr. Opin. Immunol. 19 (5), 516–521.
Hitomi, J., Katayama, T., Eguchi, Y., Kudo, T., Taniguchi, M., Koyama, Y., Manabe, T., Yamagishi, S., Bando, Y., Imaizumi, K., Tsujimoto, Y., Tohyama, M., 2004a. Involvement of caspase-4 in endoplasmic reticulum stress-induced apoptosis and Abeta-induced cell death. J. Cell Biol. 165 (3), 347–356.
Hitomi, J., Katayama, T., Taniguchi, M., Honda, A., Imaizumi, K., Tohyama, M., 2004b. Apoptosis induced by endoplasmic reticulum stress depends on activation of caspase-3 via caspase-12. Neurosci. Lett. 357 (2), 127–130.
Hu, P., Han, Z., Couvillon, A.D., Exton, J.H., 2004. Critical role of endogenous Akt/IAPs and MEK1/ERK pathways in counteracting endoplasmic reticulum stress-induced cell death. J. Biol. Chem. 279 (47), 49420–49429.
Inoue, S., Browne, G., Melino, G., Cohen, G.M., 2009. Ordering of caspases in cells undergoing apoptosis by the intrinsic pathway. Cell Death Differ. 16 (7), 1053–1061.

Jackson, W.T., Giddings Jr., T.H., Taylor, M.P., Mulinyawe, S., Rabinovitch, M., Kopito, R.R., Kirkegaard, K., 2005. Subversion of cellular autophagosomal machinery by RNA viruses. PLoS Biol. 3 (5), e156.

Jiang, B., Monroe, S.S., Koonin, E.V., Stine, S.E., Glass, R.I., 1993. RNA sequence of astrovirus: distinctive genomic organization and a putative retrovirus-like ribosomal frameshifting signal that directs the viral replicase synthesis. Proc. Natl. Acad. Sci. U. S. A. 90 (22), 10539–10543.

Jonassen, C.M., Jonassen, T.O., Saif, Y.M., Snodgrass, D.R., Ushijima, H., Shimizu, M., Grinde, B., 2001. Comparison of capsid sequences from human and animal astroviruses. J. Gen. Virol. 82 (Pt 5), 1061–1067.

Kang, J.J., Schaber, M.D., Srinivasula, S.M., Alnemri, E.S., Litwack, G., Hall, D.J., Bjornsti, M.A., 1999. Cascades of mammalian caspase activation in the yeast *Saccharomyces cerevisiae*. J. Biol. Chem. 274 (5), 3189–3198.

Koopmans, M.P., Bijen, M.H., Monroe, S.S., Vinje, J., 1998. Age-stratified seroprevalene of neutralizing antibodies to astrovirus types 1 to 7 in humans in The Netherlands. Clin. Diagn. Lab. Immunol. 5 (1), 33–37.

Kuranaga, E., Miura, M., 2007. Nonapoptotic functions of caspases: caspases as regulatory molecules for immunity and cell-fate determination. Trends Cell Biol. 17 (3), 135–144.

Li, M., Li, H., Li, C., Zhou, S., Guo, L., Liu, H., Jiang, W., Liu, X., Li, P., McNutt, M.A., Li, G., 2009. Alpha fetoprotein is a novel protein-binding partner for caspase-3 and blocks the apoptotic signaling pathway in human hepatoma cells. Int. J. Cancer 124 (12), 2845–2854.

Lowe, M., Lane, J.D., Woodman, P.G., Allan, V.J., 2004. Caspase-mediated cleavage of syntaxin 5 and giantin accompanies inhibition of secretory traffic during apoptosis. J. Cell Sci. 117 (Pt 7), 1139–1150.

MacFarlane, M., 2003. TRAIL-induced signalling and apoptosis. Toxicol. Lett. 139 (2–3), 89–97.

McLean, J.E., Ruck, A., Shirazian, A., Pooyaei-Mehr, F., Zakeri, Z.F., 2008. Viral manipulation of cell death. Curr. Pharm. Des. 14 (3), 198–220.

McStay, G.P., Salvesen, G.S., Green, D.R., 2008. Overlapping cleavage motif selectivity of caspases: implications for analysis of apoptotic pathways. Cell Death Differ. 15 (2), 322–331.

Mebratu, Y., Tesfaigzi, Y., 2009. How ERK1/2 activation controls cell proliferation and cell death: Is subcellular localization the answer? Cell Cycle 8 (8), 1168–1175.

Mendez, E., Arias, C.F., 2007. Astrovirus. In: Fields, D.N.K.B.N., Howley, P.M. (Eds.), Virology. Raven Press, New York, pp. 982–1000 (Vol. vol. 1., 2 vols).

Mendez, E., Fernandez-Luna, T., Lopez, S., Mendez-Toss, M., Arias, C.F., 2002. Proteolytic processing of a serotype 8 human astrovirus ORF2 polyprotein. J. Virol. 76 (16), 7996–8002.

Mendez, E., Salas-Ocampo, M.P., Munguia, M.E., Arias, C.F., 2003. Protein products of the open reading frames encoding nonstructural proteins of human astrovirus serotype 8. J. Virol. 77 (21), 11378–11384.

Mendez, E., Salas-Ocampo, E., Arias, C.F., 2004. Caspases mediate processing of the capsid precursor and cell release of human astroviruses. J. Virol. 78 (16), 8601–8608.

Mendez, E., Aguirre-Crespo, G., Zavala, G., Arias, C.F., 2007. Association of the astrovirus structural protein VP90 with membranes plays a role in virus morphogenesis. J. Virol. 81 (19), 10649–10658.

Mendez-Toss, M., Romero-Guido, P., Munguia, M.E., Mendez, E., Arias, C.F., 2000. Molecular analysis of a serotype 8 human astrovirus genome. J. Gen. Virol. 81 (Pt 12), 2891–2897.

Monroe, S.S., Jiang, B., Stine, S.E., Koopmans, M., Glass, R.I., 1993. Subgenomic RNA sequence of human astrovirus supports classification of Astroviridae as a new family of RNA viruses. J. Virol. 67 (6), 3611–3614.

Montero, H., Rojas, M., Arias, C.F., Lopez, S., 2008. Rotavirus infection induces the phosphorylation of eIF2alpha but prevents the formation of stress granules. J. Virol. 82 (3), 1496–504.

Moser, L.A., Schultz-Cherry, S., 2008. Suppression of astrovirus replication by an ERK1/2 inhibitor. J. Virol. 82 (15), 7475–7482.

Moser, L.A., Carter, M., Schultz-Cherry, S., 2007. Astrovirus increases epithelial barrier permeability independently of viral replication. J. Virol. 81 (21), 11937–11945.

Nakagawa, T., Zhu, H., Morishima, N., Li, E., Xu, J., Yankner, B.A., Yuan, J., 2000. Caspase-12 mediates endoplasmic-reticulum-specific apoptosis and cytotoxicity by amyloid-beta. Nature 403 (6765), 98–103.

Ramuz, O., Isnardon, D., Devilard, E., Charafe-Jauffret, E., Hassoun, J., Birg, F., Xerri, L., 2003. Constitutive nuclear localization and initial cytoplasmic apoptotic activation of endogenous caspase-3 evidenced by confocal microscopy. Int. J. Exp. Pathol. 84 (2), 75–81.

Rao, R.V., Hermel, E., Castro-Obregon, S., del Rio, G., Ellerby, L.M., Ellerby, H.M., Bredesen, D.E., 2001. Coupling endoplasmic reticulum stress to the cell death program. Mechanism of caspase activation. J. Biol. Chem. 276 (36), 33869–33874.

Riedl, S.J., Salvesen, G.S., 2007. The apoptosome: signalling platform of cell death. Nat. Rev. Mol. Cell. Biol. 8 (5), 405–413.

Schulze-Osthoff, K., Ferrari, D., Los, M., Wesselborg, S., Peter, M.E., 1998. Apoptosis signaling by death receptors. Eur. J. Biochem. 254 (3), 439–459.

Silva, M.T., do Vale, A., dos Santos, N.M., 2008. Secondary necrosis in multicellular animals: an outcome of apoptosis with pathogenic implications. Apoptosis 13 (4), 463–482.

Slee, E.A., Harte, M.T., Kluck, R.M., Wolf, B.B., Casiano, C.A., Newmeyer, D.D., Wang, H.G., Reed, J.C., Nicholson, D.W., Alnemri, E.S., Green, D.R., Martin, S.J., 1999. Ordering the cytochrome *c*-initiated caspase cascade: hierarchical activation of caspases-2, -3, -6, -7, -8, and -10 in a caspase-9-dependent manner. J. Cell Biol. 144 (2), 281–292.

Slee, E.A., Adrain, C., Martin, S.J., 2001. Executioner caspase-3, -6, and -7 perform distinct, non-redundant roles during the demolition phase of apoptosis. J. Biol. Chem. 276 (10), 7320–7326.

Stennicke, H.R., Salvesen, G.S., 1997. Biochemical characteristics of caspases-3, -6, -7, and -8. J. Biol. Chem. 272 (41), 25719–25723.

Stepczynska, A., Lauber, K., Engels, I.H., Janssen, O., Kabelitz, D., Wesselborg, S., Schulze-Osthoff, K., 2001. Staurosporine and conventional anticancer drugs induce overlapping, yet distinct pathways of apoptosis and caspase activation. Oncogene 20 (10), 1193–1202.

Strater, J., Walczak, H., Pukrop, T., Von Muller, L., Hasel, C., Kornmann, M., Mertens, T., Moller, P., 2002. TRAIL and its receptors in the colonic epithelium: a putative role in the defense of viral infections. Gastroenterology 122 (3), 659–666.

Suliman, A., Lam, A., Datta, R., Srivastava, R.K., 2001. Intracellular mechanisms of TRAIL: apoptosis through mitochondrial-dependent and -independent pathways. Oncogene 20 (17), 2122–2133.

Talanian, R.V., Quinlan, C., Trautz, S., Hackett, M.C., Mankovich, J.A., Banach, D., Ghayur, T., Brady, K.D., Wong, W.W., 1997. Substrate specificities of caspase family proteases. J. Biol. Chem. 272 (15), 9677–9682.

Taylor, M.B., Walter, J., Berke, T., Cubitt, W.D., Mitchell, D.K., Matson, D.O., 2001. Characterisation of a South African human astrovirus as type 8 by antigenic and genetic analyses. J. Med. Virol. 64 (3), 256–261.

Taylor, R.C., Cullen, S.P., Martin, S.J., 2008. Apoptosis: controlled demolition at the cellular level. Nat. Rev. Mol. Cell. Biol. 9 (3), 231–241.

Teodoro, J.G., Branton, P.E., 1997. Regulation of apoptosis by viral gene products. J. Virol. 71 (3), 1739–1746.

Tewari, M., Quan, L.T., O'Rourke, K., Desnoyers, S., Zeng, Z., Beidler, D.R., Poirier, G.G., Salvesen, G.S., Dixit, V.M., 1995. Yama/CPP32 beta, a mammalian homolog of CED-3, is a CrmA-inhibitable protease that cleaves the death substrate poly(ADP-ribose) polymerase. Cell 81 (5), 801–809.

Thornberry, N.A., Rano, T.A., Peterson, E.P., Rasper, D.M., Timkey, T., Garcia-Calvo, M., Houtzager, V.M., Nordstrom, P.A., Roy, S., Vaillancourt, J.P., Chapman, K.T., Nicholson, D.W., 1997. A combinatorial approach defines specificities of members of the caspase family and granzyme B. Functional relationships established for key mediators of apoptosis. J. Biol. Chem. 272 (29), 17907–17911.

Thornberry, N.A., Chapman, K.T., Nicholson, D.W., 2000. Determination of caspase specificities using a peptide combinatorial library. Methods Enzymol. 322, 100–110.

van Kuppeveld, F.J., Hoenderop, J.G., Smeets, R.L., Willems, P.H., Dijkman, H.B., Galama, J.M., Melchers, W.J., 1997. Coxsackievirus protein 2B modifies endoplasmic reticulum membrane and plasma membrane permeability and facilitates virus release. Embo J. 16 (12), 3519–3532.

Vandenabeele, P., Vanden Berghe, T., Festjens, N., 2006. Caspase inhibitors promote alternative cell death pathways. Sci. STKE 2006 (358), pe44.

Wang, Q.H., Kakizawa, J., Wen, L.Y., Shimizu, M., Nishio, O., Fang, Z.Y., Ushijima, H., 2001. Genetic analysis of the capsid region of astroviruses. J. Med. Virol. 64 (3), 245–255.

Wang, Z.B., Liu, Y.Q., Cui, Y.F., 2005. Pathways to caspase activation. Cell Biol. Int. 29 (7), 489–496.

Willcocks, M.M., Carter, M.J., 1993. Identification and sequence determination of the capsid protein gene of human astrovirus serotype 1. FEMS Microbiol. Lett. 114 (1), 1–7.

Wurzer, W.J., Planz, O., Ehrhardt, C., Giner, M., Silberzahn, T., Pleschka, S., Ludwig, S., 2003. Caspase 3 activation is essential for efficient influenza virus propagation. EMBO J. 22 (11), 2717–2728.

Yin, X.M., 2006. Bid, a BH3-only multi-functional molecule, is at the cross road of life and death. Gene 369, 7–19.

Yukioka, F., Matsuzaki, S., Kawamoto, K., Koyama, Y., Hitomi, J., Katayama, T., Tohyama, M., 2008. Presenilin-1 mutation activates the signaling pathway of caspase-4 in endoplasmic reticulum stress-induced apoptosis. Neurochem. Int. 52 (4–5), 683–687.